Millimetre wave SIW diplexer circuits with relaxed fabrication tolerances

John Ross Aitken[1] ✉, *Jiasheng Hong*[1], *Zhang-Cheng Hao*[2]

Q1 [1]*Institute of Sensors, Signals and Systems, Heriot-Watt University, Edinburgh, UK*
[2]*Southeast University, Nanjing, People's Republic of China*
✉ *E-mail: Ross.Aitken@TheIET.org*

Abstract: This study is concerned with the development of millimetre wave substrate integrated waveguide (SIW) diplexers, with an aim of relaxing fabrication tolerances. A method of designing SIW components initially in a dielectric filled waveguide (DWG) medium, and then translating a final optimised design to SIW is presented. Owing to the equivalence between SIW and DWG, the translated SIW components do not require a further optimisation which is a significant advantage as it speeds up the design process. The authors demonstrate this process by presenting the design of a Ka-band diplexer that consists of a highpass filter, hybrid coupler and low-order bandpass filter, where good agreement between the DWG and translated SIW cases can be observed. To investigate how the diplexer handles fabrication errors, they subjected the circuit to a tolerance analysis where simulated results suggest that the highpass filter in the diplexer is less sensitive to fabrication errors than the bandpass filter and its use in millimetre wave SIW diplexer circuits can help to relax sensitivity to fabrication errors. These observations are verified with the measurement of a fabricated Ka-band SIW diplexer, where the measured and simulated *S*-parameters are in very good agreement.

1 Introduction

There is a lot of information regarding substrate integrated waveguide (WG) (SIW) components such as filters and diplexers below millimetre wave frequencies in the literature [1]. However, when considering millimetre wave SIW diplexers, there is only a limited amount of information available. One factor in this is that above 30 GHz, component sizes are in the order of a few millimetres which makes fabrication very challenging; especially when considering that most SIW circuits use a substrate with a dielectric constant of 2 or more, making the structure even smaller when compared with the equivalent WG using air. In papers where there is a comparison between the measured and simulated results of millimetre wave SIW diplexers, there is a notable shift in the *S*-parameters as a result of fabrication tolerances. For example, in [2, 3] diplexers in the K-band part of the spectrum are presented where the shift is cited as a result of a +6 μm variation in via diameter by the authors. In [4], a diplexer operating in the V-band part of the spectrum is presented where the authors also cite fabrication tolerances as the explanation for the shift. From these discussion, it is apparent that there is a problem with fabrication tolerances in the manufacture of millimetre wave SIW diplexer circuits and relaxing the circuits' sensitivity to these tolerances would be advantageous when considering volume production.

A recent circuit topology proposed by the authors has shown that the fabrication tolerance of millimetre wave diplexer circuits can be relaxed by using a hybrid coupler/highpass filter topology in addition to a bandpass filter with full wavelength centre resonators [5, 6]. The main advantage of this topology is that the number of resonators in the diplexer circuit is halved when compared with other diplexers with a similar fractional bandwidth which relaxes the circuit sensitivity to fabrication errors. For low-cost SIW technology, tolerance issues – in particular, at millimetre wave frequencies – are more challenging to handle. Therefore, it is the purpose of this paper to demonstrate, for the first time, a proof of concept Ka-band diplexer using the hybrid coupler/highpass filter topology in SIW. It is shown that this topology can help to relax the sensitivity of millimetre wave SIW diplexer circuits to fabrication errors.

The structure of this paper is as follows. In Section 2, a method of designing SIW components is presented that consists of designing the component initially in a dielectric filled WG (DWG) medium and translating a final optimised design to SIW. Simulated results of a bandpass filter, highpass filter and hybrid coupler are shown to demonstrate the translation process. In Section 3, the design of a Ka-band SIW diplexer based on the topology proposed in [5, 6] is presented. To investigate the circuits handling of fabrication errors, simulated results of a tolerance analysis are discussed in Section 4 where changes to the via position, via diameter and dielectric constant of the substrate are considered. To validate these simulations, some promising measured results are presented in Section 5.

2 Design of SIW components

Owing to the equivalence between SIW and DWG, the design of SIW components can be carried out by designing the structure entirely in DWG and then translating a final optimised design to SIW. This method results in a faster design process, as the complete structure is optimised in DWG rather as SIW where the mesh is denser due to the vias in the model when using a commercial finite integration (FI) or finite element solver. In practise, the translation stage is carried out by splitting the component into small sections of DWG of width a_{dwg} and length z and using an equation such as that in (1) to obtain the equivalent width a_{siw} of the SIW section for a particular via separation, p and via diameter, d [7]. As the length of the section is known, the required number of vias to construct the SIW side wall can be obtained from (2), forming the new SIW component. This is summarised in Fig. 1. So long as the design guidelines in [8] are met in terms or radiation leakage and bandgap performance, the diameter and pitch of the via can be chosen arbitrarily by the designer to suit a particular component. In this way, smaller diameter vias can be selected to ensure fine details such as septum's in hybrid couplers can be realised, whereas larger diameter vias can be selected for parts of the circuit where small feature sizes are not required. Translating components in this way ensures that the SIW component matches the optimised DWG equivalent almost exactly and eliminates the need to optimise the translated SIW component entirely
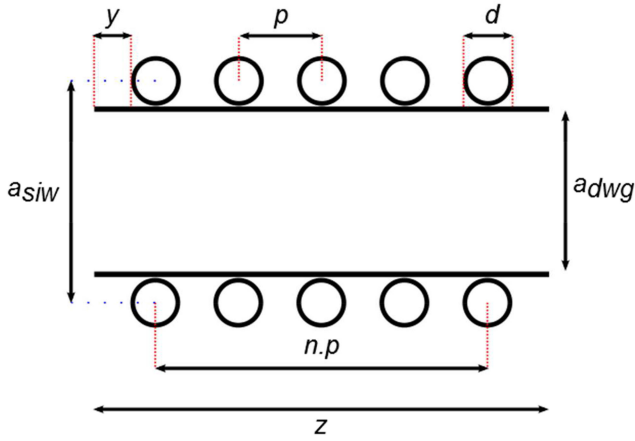
Fig. 1 *Diagram showing how the length of an SIW section, z, is related to the number of vias, n. Here, y is the distance to the edge of the section and can be chosen arbitrarily by the designer to make sure the optimum number of vias is chosen for a given p and d*
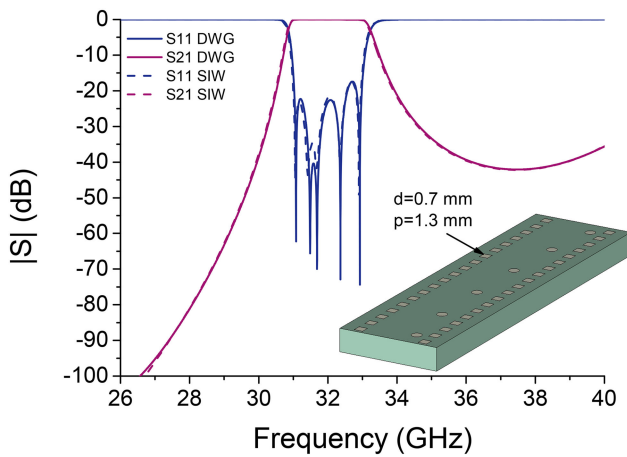

Fig. 2 *Simulated lossless response of a DWG bandpass filter and translated SIW equivalent using inductive post inverters. An RL of −15 dB is obtained over the 31–33 GHz range. There is good agreement between the SIW and DWG cases without additional optimisation of the SIW circuit. A three-dimensional (3D) image is included for reference*
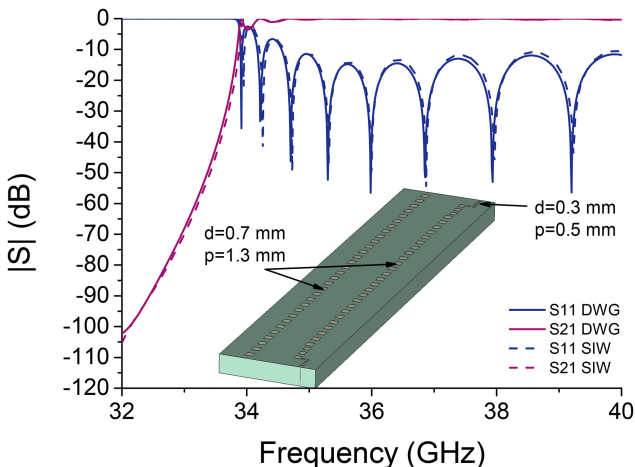

Fig. 3 *Simulated lossless response of a DWG highpass filter and translated SIW equivalent including a two section inhomogeneous transformer designed using the method in [9]. An RL of −11.5 dB is obtained over the 35.32–35.7 GHz range. There is good agreement between the SIW and DWG cases without additional optimisation of the SIW circuit. A 3D image is included for reference*

$$a_{\text{siw}} = a_{\text{dwg}} + p\left(0.766\, e^{(0.4482d/p)} - 1.176\, e^{(-1.214d/p)}\right) \quad (1)$$

$$n = \frac{z - 2y - d}{p} \quad (2)$$

To demonstrate the translation process, a bandpass filter, highpass filter and hybrid coupler are designed using the method in [6] for use with RT 5880, which has a dielectric constant of 2.2 and a height 1.574 mm. Simulated results are shown in Figs. 2–4 where both the DWG and SIW responses using lossless materials are shown for comparison. The components were simulated using the commercial FI solver CST Microwave Studio with DWG ports, where square vias were used in place of circular vias as they offer a reduced mesh density and simulation time without compromising the accuracy of the model too significantly when compared with using circular vias. Moreover, the equivalence between circular and square vias has been validated experimentally in [10, 11] for filters and couplers, respectively, with good agreement. To ensure sufficient equivalence between square and circular vias, the length of the square via, L, was determined from (3) which is based on a geometric average [12]. By comparing the simulated S-parameter response of the SIW case to the DWG case in Figs. 2–4, good agreement can be observed without a need to optimise the SIW circuit, validating the design method

$$L = d_{\text{circle}} \frac{(1/\sqrt{2}) + 1}{2} \quad (3)$$

3 SIW diplexer design

Using the components presented in Figs. 2–4, a diplexer with a similar topology to that presented in [5, 6] was designed and optimised in DWG and then translated to SIW using the method presented in Section 2. The design requirements of the diplexer can be found in Table 1 and are similar to the requirements presented in [5, 6] for backhaul communications. A diagram of the translated SIW design can be seen in Fig. 5 with the addition of elliptic bends at ports 1, 3 and 4 to facilitate the use of a WG-to-SIW transition for measurement purposes. Other types of bends such as the mitred corner bend in [13] were considered. However, due to the small septum size used to create the hybrid coupler, this type of bend would be situated too close to the bandpass filter which could result in vias overlapping during a fabrication cycle and is undesirable.

The simulated frequency response of the complete diplexer can be seen in Fig. 6 where a comparison between the optimised DWG case and translated SIW case without additional optimisation is shown. When comparing the S_{21} and S_{31} responses of the DWG and SIW cases, a small shift in frequency can be observed. This is more significant in the highpass filter where the cut-off frequency of the SIW case has shifted up in frequency by 140 MHz. This corresponds to a 0.41% shift in frequency when considering it as a percentage and can be considered negligible. The shift in frequency can be attributed to the use of square vias in the simulation where their use can only be considered as a good approximation to circular vias [12]. However, even when considering this, there is good agreement between the simulated DWG and SIW frequency responses in both channels which gives further evidence to support the design method in Section 2.

The out-of-band performance of the diplexer is limited to the bandwidth of the hybrid coupler as can be seen in Fig. 6, where interference effects are visible beyond the band edge of the highpass filter channel. Extending the useable bandwidth of the coupler will help to reduce this, improving the out-of-band performance of the diplexer for wide-band applications.

4 Tolerance analysis

To gain an understanding of how well the diplexer handles fabrication errors, a tolerance study was conducted where it was assumed the vias would be drilled using a printed circuit board (PCB) drilling machine and then plated using a conductive material. Three separate cases are investigated: an error in the positioning of the vias, an error in the dielectric constant of the
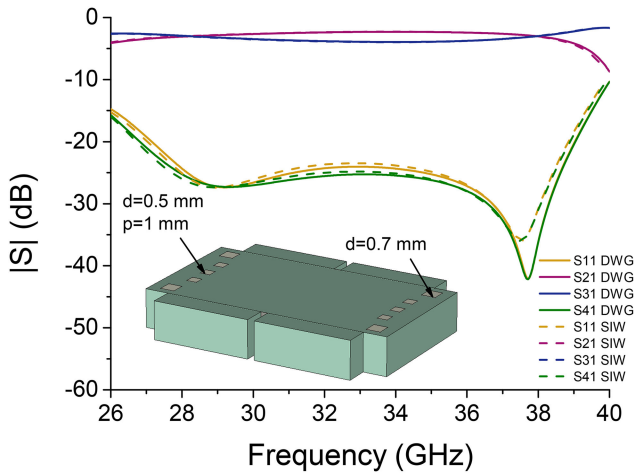
Fig. 4 *Simulated lossless response of a DWG hybrid coupler and the translated SIW equivalent. An RL of −20 dB in addition to a ±0.84 dB variation in S$_{21}$ and S$_{31}$ is obtained over the 27–38.8 GHz range. There is good agreement between DWG and SIW cases without additional optimisation of the SIW circuit. A 3D image is included for reference*
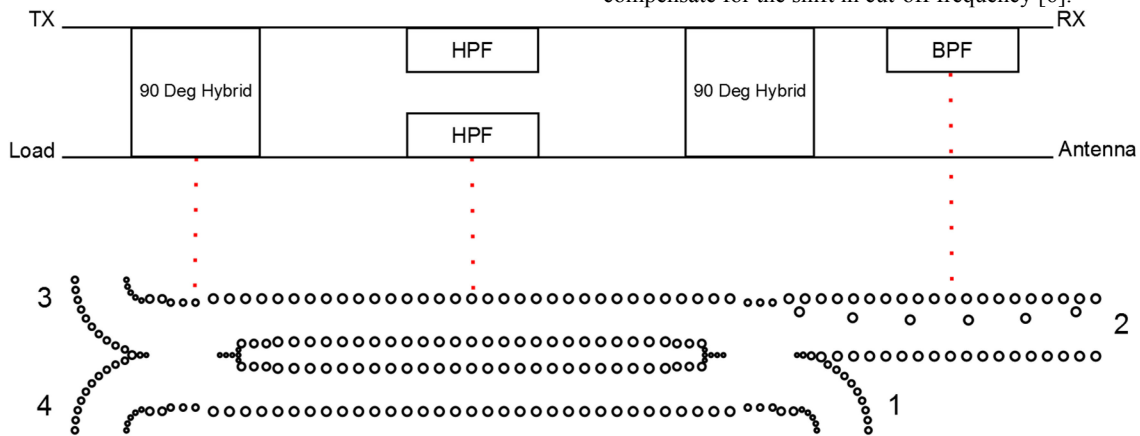

Fig. 5 *Schematic diagram of the SIW diplexer circuit. To facilitate the use of a WG-to-SIW transition, elliptic bends were added to ports 1, 3 and 4*

[14]. This can result in overlapping of the vias which is undesirable, and ultimately limits the via separation that can be used to construct SIW side walls. To investigate how this affects the diplexer response, the positions of the vias were altered by ±0.04 mm over 20 samples for both variations in the *x* and *y* planes. The simulated frequency response can be seen in Figs. 7 and 8 for both cases.

By comparing Figs. 7 and 8, changes to the via position in the *y*-axis appear to affect the diplexer response less than changes to the via position in the *x*-axis. This is expected, as the cut-off frequency of the SIW and subsequently the guide wavelength of the SIW is related to changes in the width for the fundamental mode. Moreover, this sensitivity is further demonstrated in Fig. 7, where the cut-off frequency of the highpass filter has a shift of $^{+340}_{-470}$ MHz. However, the return loss (RL) in the highpass filter channel appears to be stable and does not fall below −15 dB in the passband of the highpass filter. This is not true for the bandpass filter, where the RL varies more significantly as a consequence of the bandwidth changing. This suggests that the highpass filter is less sensitive to variations in the via position than the bandpass filter. Designing the highpass filter so that the cut-off frequency is sufficiently far enough away from the passband of channel 2 would compensate for the shift in cut-off frequency [6].

substrate, and an error in the via diameter. A discussion of each case will now follow.

4.1 Error in via position

Q2 The CNC drilling process is a popular fabrication method for drilling vias in SIW due to the quick production turnaround that can be achieved. In addition, extremely small via holes are achievable with a reasonable positional accuracy. For example, in [14] vias of 0.1 mm in diameter were demonstrated on a 0.1 mm thickness glass fibre laminate substrate. To ensure high-precision drilling with low drill breakage, the CNC drilling process drives the drill bit into the substrate with a high rotational speed which can be on the order of 300 krpm [15]. In this case, centripetal forces rotate the drill in such a way that the positional error in the entry point of the drill on the substrate can be as large as ±0.04 mm

4.2 Error in dielectric constant

Changes to the dielectric constant affect the cut-off frequency and guide wavelength of the SIW. In this case, choosing a substrate that has a low variation in the dielectric constant is essential. Some discussion are given in [16] where it is suggested that Rogers RT 5880 has the lowest variation in dielectric constant of ±0.02, in addition to having the lowest dielectric loss which is essential for millimetre wave applications. Moreover, this substrate is isotropic and the variation in dielectric constant is quoted up to 40 GHz which justifies the use of RT 5880 for this design [17]. To investigate how a change to the dielectric constant affects the diplexers frequency response, the dielectric constant was varied by ±0.02 over 20 samples. The simulated frequency response can be seen in Fig. 9 where a shift in frequency can be observed. The bandpass filter appears to be more sensitive to variations in the dielectric constant than the highpass filter due to the degraded bandwidth and RL. This suggests that the highpass filter is less sensitive to variations in the dielectric constant than the bandpass filter as the RL of the highpass filter remains stable. This is expected as the length of each resonator in the bandpass filter is a function of the guide wavelength. Therefore, any change in the dielectric constant will significantly alter the frequency response of the bandpass filter. These observations signify there is a need for the continued development of high-frequency substrates: further reducing the ±0.02 variation in the dielectric constant will reduce the observed shift in frequency.
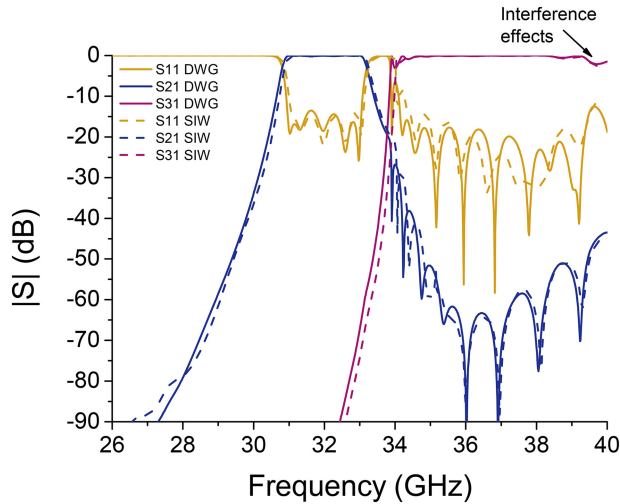
Table 1 Design specifications for the SIW diplexer circuit. The specifications for this design are based on those in [5, 6] for backhaul communications. However, to facilitate the proof of concept design, some requirements have been relaxed

Channel 1		Channel 2	
Passband	31.00–33.00 GHz	Passband	35.32–37.50 GHz
SB rejection	−55 dB between 35.32 and 37.5 GHz	SB rejection	−60 dB between 31.00 and 33.00 GHz
RL	−14 dB	RL	−14 dB
IL	−2 dB	IL	−2 dB

Fig. 6 *Simulated lossless response of a DWG diplexer and the translated SIW equivalent. There is good agreement between the DWG and SIW cases without additional optimisation of the SIW circuit*
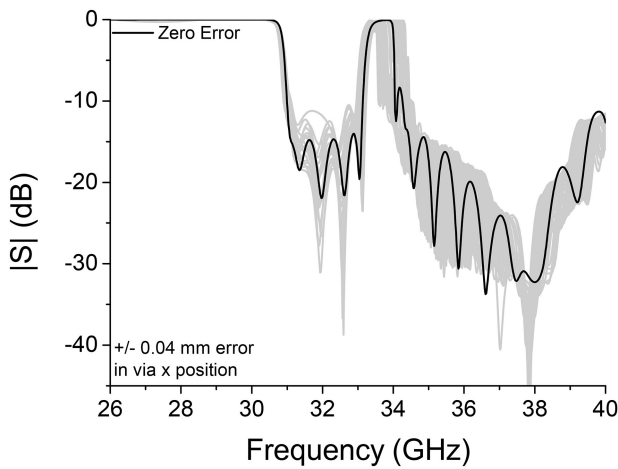

Fig. 7 *Simulated S_{11} frequency response of the diplexer using lossless materials with a ±0.04 mm variation in via x-position over 20 samples*
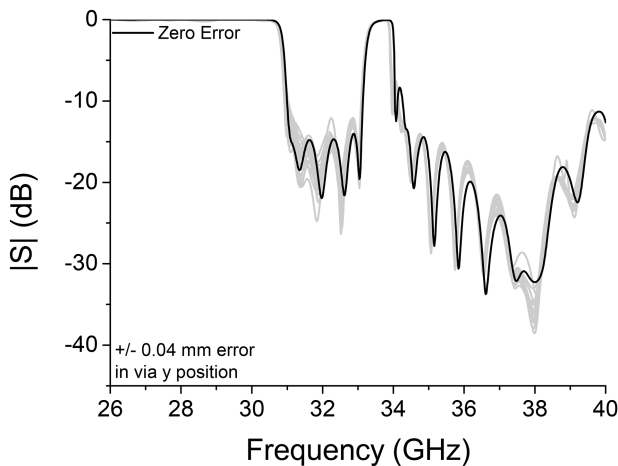

Fig. 8 *Simulated S_{11} frequency response of the diplexer using lossless materials with a ±0.04 mm variation in via y-position over 20 samples*

4.3 Error in via diameter

Drilling through PCB substrates ultimately wears out the drill cutters. In [14], it was shown that this wear is related to the position on the drill cutter, where more wear is experienced closer to the tip of the drill. In this case, it was reported that the tip of the drill can be −0.025 mm smaller than new drills over a production cycle. This is undesirable as reducing the via diameter has the

effect of shifting the diplexing response down in frequency as the width and length of each SIW component are made larger [16]. Additionally, due to the high rotational speed of the drill, loose substrate laminate material can heat up and bond to the drill which further affects the diameter of the via hole [15]. In this case, replacing worn drills would help to ensure a clean via is produced. Another factor in the diameter of via holes is the aspect ratio. For example, due to the centripetal forces acting on the drill, the entry hole will be larger than the exit hole as the drill enters the substrate at a slight angle [14]. This is more significant on smaller diameter drills, and is related to the thickness of the substrate being processed. Ultimately, this limits the substrate thicknesses which can be processed to ensure acceptable aspect ratios are achieved. Taking into account all variables related to the diameter of the via hole, predicting how the circuit will react due to a change in via diameter is difficult as the model is inherently complex. To investigate how changes to the via diameter affect the diplexer, a simplified model was used where the diameters of the entry and exit holes were changed systematically. Although a simplification, this model takes into account the reduction in via diameter due to the wearing of the drill cutters, and the larger entry hole of the via due to the drill entering at an angle. The simulated results can be seen in Fig. 10 where the via diameter was varied by ±0.025 mm over 20 samples. As changes to the via diameter affect the equivalent width of the SIW, a shift in the cut-off frequency of the highpass filter and bandpass filter can be observed. The shift appears to be more significant in the bandpass filter, where a change to the filters bandwidth and RL can be seen. In contrast to this, the RL of the highpass filter is stable in the passband of channel 2 and does not reduce below −15 dB. This suggests that the highpass filter is less sensitive to variations in the via diameter than the bandpass filter.

5 Measured performance of the SIW diplexer

A photograph of the fabricated diplexer can be seen in Fig. 11 along with a comparison between measured and simulated results in Fig. 12. The measured passband of the bandpass channel was found to be 30.62–32.72 GHz, whereas the measured cut-off frequency of the highpass channel was found to be 33.63 GHz. This corresponds to a shift of −350 and −430 MHz. It should be noted that the measured bandwidth of the bandpass filter is 6.63% which is marginally larger than the desired 6.25%. In this case, more energy is passing through the filter which can only be attributed to a positive error in the via x–position, a reduction in via diameter, or a combination of both. Assuming that these errors are systematic during the diplexers fabrication, the shift in cut-off frequency of the highpass filter can also be attributed to these errors. To confirm this, the average via diameter, pitch and width of the highpass filter section was measured using a digital microscope. The measured results can be found in Fig. 13 and are in agreement with the discussion above in addition to the predicted range of the tolerance analysis in Section 4.

When comparing the measured and simulated RL of channel 2, there is good agreement between the two cases, even when considering the downshift in frequency. However, this is not true for the RL of channel 1 where the shift in frequency degrades the passband RL too significantly. This suggests that the highpass filter is less sensitive to fabrication errors than the bandpass filter, and justifies its use in helping to relax fabrication tolerances within the diplexer.

A summary of the measured diplexers performance neglecting the downshift in frequency can be found in Table 2 for ease of reading. When comparing Table 2 to the desired specifications in Table 1, it can be seen that the diplexer would narrowly fail to meet the requirements for RL in channel 1, and stopband (SB) performance in both channel 1 and channel 2 if there was no shift in frequency. The differences between the measured and simulated SBs can be attributed to interference in the coupling region, where reflected TX and RX signals can interfere with the SB. For Q2example, consider the deviations between the measured and Q2simulated S_{21} and S_{31} responses over the 35–40 and 26–32 GHz ranges, respectively, where effects of destructive and constructive
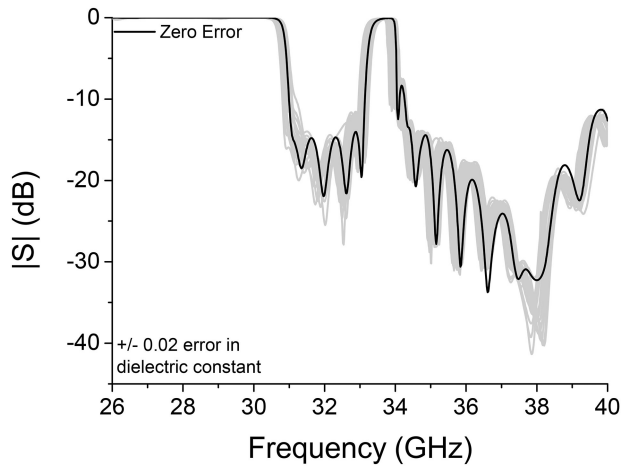
Fig. 9 *Simulated S_{11} frequency response of the diplexer using lossless materials with a ±0.02 variation in the dielectric constant over 20 samples*
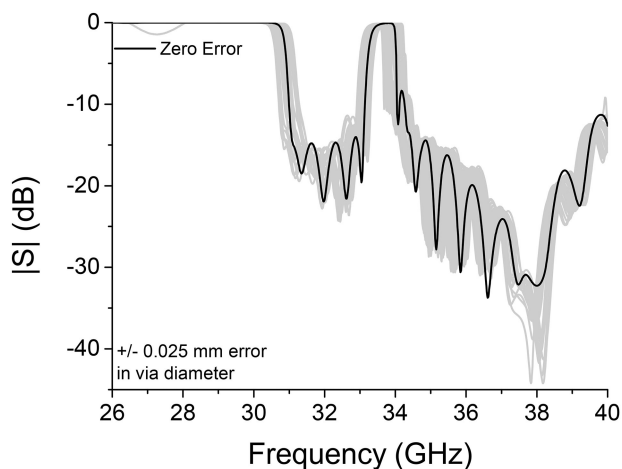

Fig. 10 *Simulated S_{11} frequency response of the diplexer using lossless materials with up to a ±0.025 mm reduction in via diameter over 20 samples*
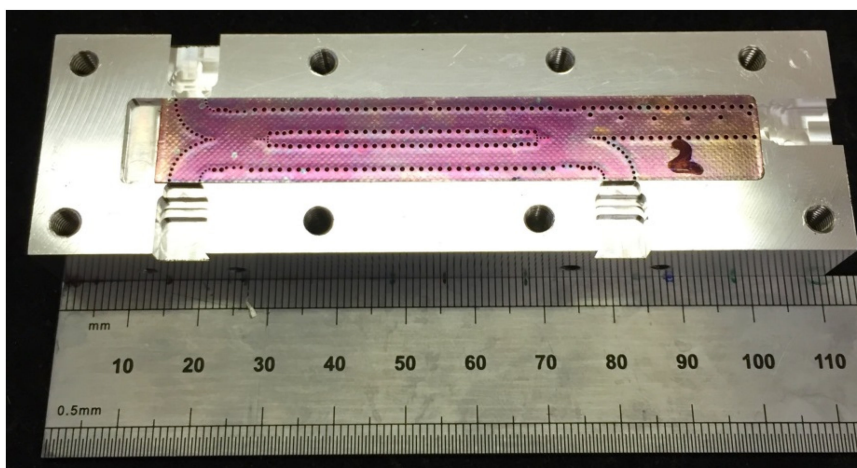

Fig. 11 *Photograph of the fabricated SIW diplexer situated inside an aluminium alloy WG housing. A flat lid is used to complete the circuit. Additionally, the diplexer is excited using a WG-to-SIW transition where the ports on the diplexer are matched to a standard WG 22 flange. The design of the WG-to-SIW transition is detailed in [18]*

interferences can be observed. In this case, increasing the number of steps in the coupling region will improve the couplers isolation which will subsequently help to improve the SBs of the bandpass and highpass filters [6]. Nevertheless, as a proof of concept design, the results are promising. For example, by considering the diplexers in [2–4], the measured insertion loss (IL) for this design is considerably less than the current state of the art. However, further work is required to relax the sensitivity of SIW bandpass filters to fabrication errors if SIW diplexers are to be used for commercial millimetre wave applications such as backhaul.

6 Conclusions

This paper has concerned itself with the design of millimetre wave SIW diplexer circuits with an aim of improving tolerance handling ability. A method of designing SIW components initially in a DWG medium and then translating a final optimised design to SIW is presented. Owing to the equivalence between SIW and DWG, the translated SIW components do not require a further optimisation which is a significant advantage as it speeds up the design process. We demonstrated this method by showing simulated results of a Ka-band bandpass filter, highpass filter and hybrid coupler where good agreement is observed between the original DWG response and the translated SIW response. Using these components, we present the design of a Ka-band SIW diplexer based on the topology proposed in [5, 6]. To gain an understanding of how fabrication errors will affect the diplexers frequency response, we carried out a tolerance analysis where errors in the via position, dielectric constant, and via diameter were studied in detail. These observations suggest that the highpass filter in the diplexer is less sensitive to fabrication errors than the bandpass filter and its use in the diplexer help to relax fabrication errors. We validated these simulations by fabricating the Ka-band SIW diplexer using RT 5880 where good agreement is observed between the measured and simulated frequency responses. However, the results suggest that further work is required in relaxing the fabrication tolerance of SIW bandpass filters if SIW diplexers are to be used for commercial millimetre wave applications such as backhaul.
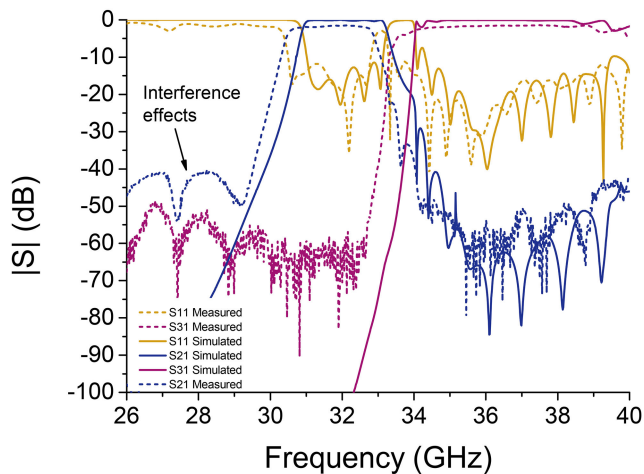
7 Acknowledgment

Fig. 12 *Simulated lossless and measured performance of the SIW diplexer using a WG-to-SIW transition*
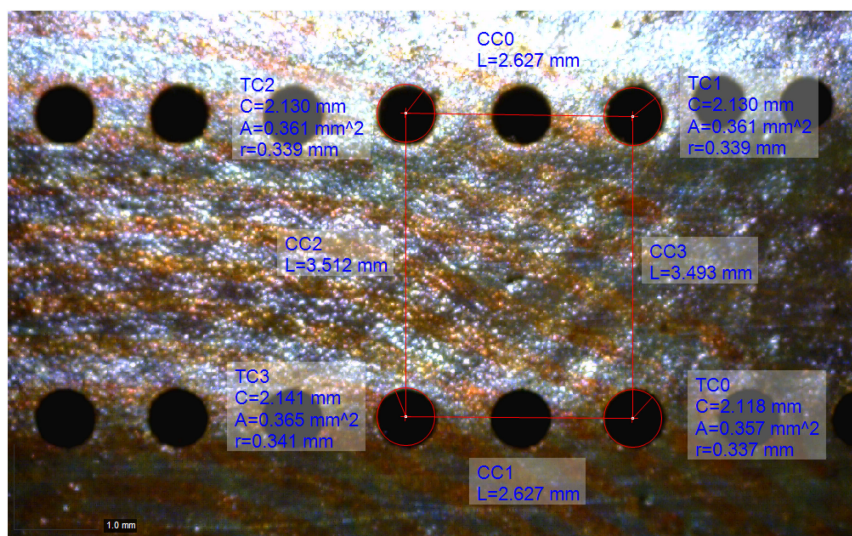

Fig. 13 *Microscope image of a highpass filter section. The average via diameter was measured to be 0.68 mm which is smaller than the 0.7 mm design value. Conversely, the via pitch was measured to be 1.32 mm which is larger than the 1.3 mm design value. The average width of the highpass filter section was found to be 3.5 mm which is larger than the 3.46 mm design value. These values are in line with the tolerance analysis in Section 4 and validate the method*

Table 2 Summary of the measured diplexers performance. Maximum IL is given at the centre frequency of the shifted passbands; moreover, the RL and SB performance are given as the minimum value in the shifted passbands

Channel 1			Channel 2		
IL, dB	RL, dB	SB, dB	IL, dB	RL, dB	SB, dB
−1.63	−11.8	−50.7	−1.60	−16.2	−56.8

8 References

[1] Bozzi, M., Georgiadis, A., Wu, K.: 'Review of substrate-integrated waveguide circuits and antennas', *IET Microw. Antennas Propag.*, 2011, **5**, (8), p. 909

[2] Kordiboroujeni, Z., Bornemann, J.: 'Mode matching design of substrate integrated waveguide diplexers'. Proc. MTT-S Int. Microwave Symp. Digest, Seattle, Washington, 2013, pp. 1–3

[3] Kordiboroujeni, Z., Bornemann, J., Sieverding, T.: 'K-band substrate integrated waveguide T-junction diplexer design by mode-matching techniques'. Proc. Asia-Pacific Microwave Conf., Sendai, Japan, 2014, pp. 1297–1299

[4] Athanasopoulos, N., Makris, D., Voudouris, K.: 'A 60 GHz planar diplexer based on substrate integrated waveguide technology', *Act. Passive Electron. Compon.*, 2013, **2013**

Q3 [5] Aitken, J.R., Hong, J.: 'Tolerance considerations for wireless backhaul diplexer circuits'. Proc. 44th European Microwave Conf., Rome, 2014, pp. 620–623

[6] Aitken, J.R., Hong, J.: 'Design of millimetre wave diplexers with relaxed fabrication tolerances', *IET Microw. Antennas Propag.*, 2015, **9**, (8), pp. 802–807

[7] Kordiboroujeni, Z., Bornemann, J.: 'Designing the width of substrate integrated waveguide structures', *IEEE Microw. Wirel. Compon. Lett.*, 2013, **23**, (10), pp. 518–520

[8]   Chen, X.-P., Wu, K.: 'Substrate integrated waveguide filter: basic design rules and fundamental structure features', *IEEE Microw. Mag.*, 2014, **15**, (5), pp. 108–116

[9]   Bandler, J.W.: 'Computer optimization of inhomogeneous waveguide transformers', *IEEE Trans. Microw. Theory Tech.*, 1969, **17**, (8), pp. 563–571

[10]   Kordiboroujeni, Z., Taringou, F., Bornemann, J.: 'Efficient mode-matching design of substrate-integrated waveguide filters'. Proc. 42nd European Microwave Conf., Amsterdam, 2012, pp. 253–256

[11]   Kordiboroujeni, Z., Bornemann, J., Sieverding, T.: 'Mode-matching design of substrate-integrated waveguide couplers'. Proc. Asia-Pacific Symp. on Electromagnetic Compatibility, Singapore, 2012, pp. 701–704

[12]   Buchta, M., Heinrich, W.: 'On the equivalence between cylindrical and rectangular via-holes in electromagnetic modeling'. Proc. 37th European Microwave Conf., Munich, 2007, pp. 142–145

[13]   Kordiboroujeni, Z., Bornemann, J.: 'Mode-matching analysis and design of substrate integrated waveguide T-junction diplexer and corner filter', *Int. J. Numer. Model., Electron. Netw. Devices Fields*, 2015, **28**, (5), pp. 497–507

[14]   Watanabe, H., Tsuzaka, H., Masuda, M.: 'Microdrilling for printed circuit boards (PCBs) – influence of radial run-out of microdrills on hole quality', *Precis. Eng.*, 2008, **32**, (4), pp. 329–335

[15]   Zheng, L., Wang, C., Yang, L.*, et al.*: 'Characteristics of chip formation in the micro-drilling of multi-material sheets', *Int. J. Mach. Tools Manuf.*, 2012, **52**, (1), pp. 40–49

[16]   Chen, X.-P., Wu, K.: 'Substrate integrated waveguide filters: practical aspects and design considerations', *IEEE Microw. Mag.*, 2014, **15**, (7), pp. 75–83

[17]   https://www.rogerscorp.com, accessed 04 June 2016

[18]   Aitken, J.R., Hong, J.: 'Millimetre wave wideband low-loss waveguide-to-substrate integrated waveguide transition', *Microw. Opt. Technol. Lett.*, 2017, **59**, (1), pp. 10–12